THE JOURNAL OF PHYSICAL CHEMISTRY A

ARTICLE

pubs.acs.org/JPCA

Geometry and Spectral Properties of the Protonated Homodimer of Pyridine in the Liquid and Solid States. A Combined NMR, X-ray Diffraction and Inelastic Neutron Scattering Study

S. Kong,[†] A. O. Borissova,[‡] S. B. Lesnichin,[†,§] M. Hartl,[∥] L. L. Daemen,[∥] J. Eckert,[⊥] M. Yu. Antipin,[‡] and I. G. Shenderovich*[,†,§]

[†]Institut für Chemie und Biochemie, Freie Universität Berlin, Takustrasse 3, 14195 Berlin, Germany

[‡]A.N. Nesmeyanov Institute of Organoelement Compounds, Russian Academy of Sciences, 119991, Vavilov Street, 28, Moscow, Russian Federation

[§]Department of Physics, St. Petersburg State University, Ulianovskaya 1, 198504 St. Petersburg, Russian Federation

[∥]Lujan Center, Los Alamos National Laboratory, Los Alamos, New Mexico 87545, United States

[⊥]Department of Chemistry, University of South Florida, 4202 East Fowler Avenue, Tampa, Florida 33620, United States

Supporting Information

ABSTRACT: The structure and spectral signatures of the protonated homodimer of pyridine in its complex with a poorly coordinating anion have been studied in solution in $CDF_3/CDClF_2$ down to 120 K and in a single crystal. In both phases, the hydrogen bond is asymmetric. In the solution, the proton is involved in a fast reversible transfer that determines the multiplicity of NMR signals and the sign of the primary H/D isotope effect of −0.95 ppm. The proton resonates at 21.73 ppm that is above any value reported in the past and is indicative of a very short hydrogen bond. By combining X-ray diffraction analysis with model computations, the position of the proton in the crystal has been defined as d(N−H) = 1.123 Å and d(H···N) = 1.532 Å. The same distances have been estimated using a ^{15}N NMR correlation. The frequency of the protonic out-of-plane bending mode is 822 cm^{-1} in agreement with Novak's correlation.

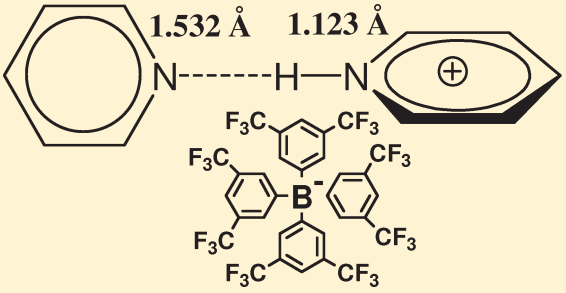

1. INTRODUCTION

A detailed understanding of the relationship between spectral parameters and the structure of strong hydrogen bonds is crucial for the elucidation of reaction pathways in many chemical and biological systems.[1] Homoconjugated ions of $[A\cdots H\cdots A]^-$ and $[B\cdots H\cdots B]^+$ types are benchmark systems of strong hydrogen bonds, since the proton affinities of the partners are the same.[2−4] Despite the formal symmetry of these complexes the location of the mobile proton depends on the electronegativity of the hydrogen-bonded heavy atoms,[2] on steric hindrance,[5−7] and the environment.[8] The hydrogen bond geometry in the condensed state is affected by the temperature dependent solvent polarity,[9−12] coupled hydrogen bonds,[13,14] and by the crystal field.[15,16] The hydrogen bifluoride ion, $[FHF]^-$, is known to possess the strongest (about 200 kJ/mol[17−19]) hydrogen bond. This ion is characterized by a symmetric structure $D_{\infty h}$[20−23] in the gas phase and in solution, where the F...F distance appears to depend slightly on the polarity of the solvent.[24] The symmetry of $[FHF]^-$ may be lifted by an interaction with the counterion.[25] The Eigen and Zundel ions are other rather well-known examples.[26,27] They have been the subject of intense research efforts with the aim to understand the microscopic mechanisms governing proton transfer in water.[28] The interpretation of their spectral properties in the condense phase is far from trivial, as it cannot be assumed that these species are decoupled from the environment.[29,30]

The present study deals with the protonated homodimer of pyridine, $[Pyr\cdots H\cdots Pyr]^+$. This system is well studied. Theoretical calculations on this complex predict an N...N distance of 2.64 Å.[31] The hydrogen bond is linear and asymmetric even in the absence of external interactions[2,32,33] with the barrier for proton transfer about 4 kJ/mol.[32] Thus, this complex exhibits a typical example of the so-called proton-sharing[34] or low-barrier[35] hydrogen bonds. The aromatic rings are oriented perpendicular to each other. In the solid state, the interaction with the counterion perturbs the linearity of the bond and results in a lengthening of the hydrogen bond. The shortest known N...N distance of 2.655 Å was found in the compound $[(Pyr)_2H]_2^{2+}[P_2S_8]^{2-}$.[36] However, the fact that the angle between the C_2 symmetry axes of the pyridines in this complex is 169° indicates

Received: April 15, 2011
Revised: June 6, 2011
Published: June 06, 2011

ACS Publications © 2011 American Chemical Society

that the total length of the $[Pyr\text{-}H\cdots Pyr]^+$ hydrogen bond should in fact be longer. The only available neutron diffraction study on $[Pyr\text{-}H\cdots Pyr]^+$ reported an N...N distance of 2.737 Å, a H-bond angle of 172°, N−H and H···N distances of 1.086 and 1.658 Å, respectively, so that the total length of the $[N\text{-}H\cdots N]^+$ hydrogen bond is 2.744 Å.[37] X-ray structural analysis of other crystals gave N...N distances above 2.73 Å.[38−40] The $[N\text{-}H\cdots N]^+$ hydrogen bond can be shorter for substituted pyridines. In the case of 4-aminopyridine, it was found to be about 2.7 Å[41,42] but still asymmetric. The most important feature in IR spectra of $[Pyr\text{-}H\cdots Pyr]^+$ in solution is a strong, broad doublet at 2080 and 2530 cm^{-1}. The splitting was attributed to a Fermi resonance between the N−H stretching and a combination vibration. It was assumed that the latter included the N−H bending vibration and a ring vibration.[43,44] Alternatively, it could be a result of proton tunneling in a double minimum potential.[45] The same pattern has also been observed for substituted pyridines.[46]

In this communication we aim to eliminate problems arising from the effect of the counterion on the hydrogen bond geometry, by examining the structural and spectral properties of $[Pyr\text{-}H\cdots Pyr]^+$ in a polar aprotic solvent as well as in the solid state in a complex with a very bulky poorly coordinating tetrakis[3,5-bis(trifluoromethyl)phenyl]-borate ($[BArF]^-$) as the counteranion. On the basis of our previous studies we expect, that $[BArF]^-$ cannot affect the geometry of the homoconjugated cation to a significant degree.[47,48] Experimental results obtained for $[Pyr\text{-}H\cdots Pyr]^+$ $[BArF]^-$ can therefore be better compared to theoretical calculations to improve their interpretation and to elucidate the effect of external interactions. Four types of measurements are necessary to reach our goal: (i) the ^1H and ^{15}N nuclear magnetic resonance (NMR) spectral properties of $[Pyr\text{-}H\cdots Pyr]^+$ in the polar freon mixture $CDF_3/CDClF_2$ as solvent as it is liquid down to 100 K, which makes it possible to observe hydrogen bonded complexes in the slow exchange regime,[49] (ii) characterization of the crystal structure of $[Pyr\text{-}H\cdots Pyr]^+$ $[BArF]^-$ using high-resolution X-ray diffraction analysis (XRD), (iii) inspection of the ^{15}N NMR spectral properties of $[Pyr\text{-}H\cdots Pyr]^+$ in the polycrystalline state, and (iv) analysis of the mobile hydron dynamics in $[Pyr\text{-}H\cdots Pyr]^+$ in the polycrystalline state using vibrational spectroscopy by inelastic neutron scattering (INS).

This paper is organized as follows. After an experimental section the experimental results are described. This is followed by our interpretation of the obtained results and a discussion of the relationship between spectroscopic parameters and the structure of the hydrogen bond in the $[Pyr\text{-}H\cdots Pyr]^+$ cation.

2. EXPERIMENTAL SECTION

2.1. Materials. All chemicals were purchased from Sigma-Aldrich and used without additional purification. Deuterated solvents and ^{15}N-enriched pyridine were purchased from Eurisotop (Germany). The deuterated freon gas mixture $CDF_3/CDClF_2$ for the low-temperature NMR experiments, whose composition varied between 1:2 and 1:3, was prepared from chloroform-d_1 as described recently.[49]

Preparation of $[Pyr\text{-}H\cdots Pyr]^+$ $[BArF]^-$ Crystals. Pyridine (175.2 μL,172 mg), 37% HCl (86.4 μL, 102.8 mg), and $[BArF]^-$ Na^+ (939.6 mg) were dissolved in water and stirred overnight. The precipitate was filtrated and dried under vacuum. The powder was crystallized in solution of CH_2Cl_2/Hexan. Pyridine-^{15}N was used for the samples utilized in NMR experiments. DCl was used to obtain $[Pyr\text{-}D\cdots Pyr]^+$ $[BArF]^-$ species.

2.2. NMR Measurements. Liquid-state ^1H and ^{15}N NMR spectra were measured on a Bruker AMX 500 spectrometer operated at 11.7 T equipped with a probe-head enabled to perform experiments down to 100 K. The solvent used was a liquefied deuterated freon gas mixture $CDF_3/CDClF_2$. The ^1H spectra were indirectly referenced to tetramethylsilane (TMS) by setting the central component of the residual $CHClF_2$ triplet of the freon mixture to 7.18 ppm.[49] The ^{15}N spectra were indirectly referenced to pyridine dissolved in $CDF_3/CDClF_2$ (0 ppm). Bulk pyridine resonates at 277.6 ppm with respect to external solid $^{15}NH_4Cl$ and at −63.6 ppm with respect to external liquid nitromethane if the following relation $\delta(CH_3{}^{15}NO_2,\ liq.) = \delta(^{15}NH_4Cl,\ solid) - 341.2$ ppm[50,51] is taken into account. The standard ^1H and inverse-gated ^1H-decoupled ^{15}N NMR spectra were recorded with recycle times of 3 and 5 s, respectively.

The solid-state ^{15}N NMR measurements were performed on a Bruker MSL−300 instrument operated at 7 T, equipped with a variable-temperature Chemagnetics-Varian 6 mm pencil CPMAS probe. The samples were spun at 8 kHz under the magic-angle-spinning (MAS) conditions. The $\{^1H\}$-^{15}N CPMAS spectra were recorded using a cross-polarization contact time of 5 ms, the typical 90°-pulse lengths were about 4.0 μs. The ^{15}N spectra were indirectly referenced to bulk liquid pyridine (0 ppm).

2.3. XRD Measurements. X-ray diffraction data for single $[Pyr\text{-}H...Pyr]^+$ $[BArF]^-$ crystals were collected using a "Bruker SMART APEX2" CCD diffractometer. The obtained images were integrated to determine the precise unit cell dimensions and margin of error.[52] The absorption correction was applied semi-empirically using the SADABS program.[53] The crystals of the complex (M = 1022.43) were monoclinic, space group $P2_1/n$, at 193 ± 2 K: a = 13.1238(14) Å, b = 18.615(3) Å, c = 18.123(3) Å, β = 100.884(3)°, V = 4347.7(11) Å^3, Z = 4, d_{calc} = 1.562 g.cm^{-3}, μ(MoKα) = 1.64 cm^{-1}, F(000) = 2040. Intensities of 30 578 reflections were measured and 10 477 independent reflections [R_{int} = 0.0604] were used in further refinement. The refinement converged to wR2 = 0.2342 and GOF = 1.345 for all independent reflections ($R1$ = 0.1338 was calculated against F for 4895 observed reflections with $I > 2\sigma(I)$). Initially spherical atom refinements were undertaken with the SHELXTL PLUS 5.0 code using the full-matrix least-squares method.[54] All non-hydrogen atoms were refined with anisotropic thermal parameters. A relatively low quality of the obtained data was due to the heavily disordered fluorine atoms of CF_3 groups. Fluorine atoms of these groups were described using the AFIX 127 command as two components rotated by 60° with their population refined as a free variable. The best description in this case would probably be a toroid with the three fluorine atoms delocalized along a circle around the carbon atom, but the program package used does not imply such opportunity. The atomic coordinates, the bond lengths, the angles, and the thermal parameters have been deposited at the Cambridge Crystallographic Data Centre (CCDC) with number 784456.

2.4. Inelastic Neutron Scattering Measurements. Inelastic neutron scattering spectra were obtained on the inverse geometry Filter Difference Spectrometer[55] of the Lujan Center at Los Alamos National Laboratory. Approximately 2 g of $[Pyr\text{-}H\cdots Pyr]^+$ $[BArF]^-$ was loaded in an Al sample container under He atmosphere for data collection at 10 K. The material was subsequently recrystallized in CH_3OD to exchange the H-bond proton with deuterium. An equivalent INS spectrum

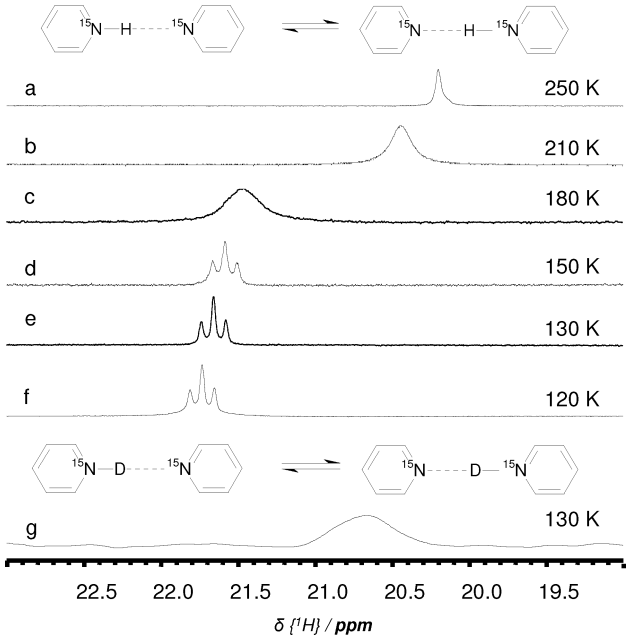

Figure 1. The low-field part of ^{1}H NMR spectra of $[Pyr\text{-}H\cdots Pyr]^{+}$ at different temperatures (a−f) and of a ^{2}H NMR spectrum of $[Pyr\text{-}D\cdots Pyr]^{+}$ at 130 K (g) in $CDF_3/CDClF_2$ with $[BArF]^{-}$ as counteranion.

Table 1. NMR Parameters of $[Pyr\text{-}H\cdots Pyr]^{+}$ in $CDF_3/CDClF_2$

T, K	δ(^{1}H), ±0.01 ppm	δ(^{2}H), ±0.05 ppm	δ(^{15}N), ±0.1 ppm	|J(^{15}N^{1}H)|, ±0.5 Hz
250	20.20			
210	20.44		−63.6	
180	21.47		−62.7	
150	21.58		−62.7	39.9
130	21.67	20.72		39.9
120	21.73		−62.7	40.4

was then collected with $[Pyr\text{-}D\cdots Pyr]^{+}$ $[BArF]^{-}$ with the aim of obtaining a spectral difference. This process can eliminate most of the vibrational bands from Pyr and $[BArF]^{-}$ modes except for those, of course, that are strongly coupled to displacements of the H-bond proton.

3. RESULTS

3.1. Liquid State ^{1}H, ^{2}H, and ^{15}N NMR. The low-field parts of ^{1}H NMR spectra of $[Pyr\text{-}H\cdots Pyr]^{+}$ in $CDF_3/CDClF_2$ with $[BArF]^{-}$ as the counteranion measured at low temperatures are depicted in Figure 1. The main NMR parameters extracted from the spectra are collected in Table 1. The chemical shift of the resonance attributed to the mobile proton depends on temperature. This effect is especially pronounced above 180 K and is accompanied by a loss of the signal splitting.[56] This type of transition is indicative for an intermolecular proton exchange. Water completely precipitates from $CDF_3/CDClF_2$ below 170 K.[57] Thus, the proton exchange above 180 K is mostly promoted by the residual water. Below 150 K the signal is a triplet with a coupling constant of |40| Hz. At 130 K, the triplet is located at 21.67 ppm. ^{2}H NMR spectrum of $[Pyr\text{-}D\cdots Pyr]^{+}$ displays at 130 K a broad peak at 20.72 ppm. That is the primary isotope effect on the NMR chemical shift at 130 K is $^{p}\Delta(H/D) \equiv \delta(N\underline{D}N) - \delta(N\underline{H}N) = -0.95$ ppm.

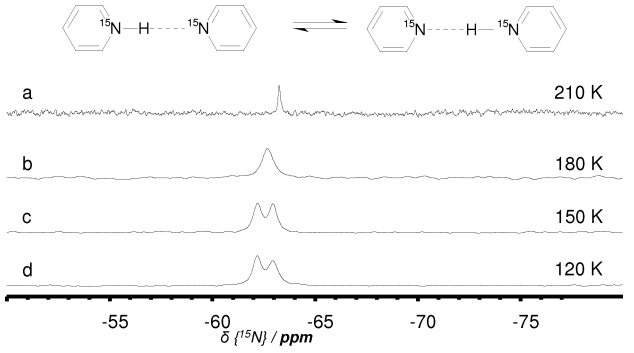

Figure 2. ^{15}N NMR spectra of $[Pyr\text{-}H\cdots Pyr]^{+}$ in $CDF_3/CDClF_2$ with $[BArF]^{-}$ as counteranion at different temperatures.

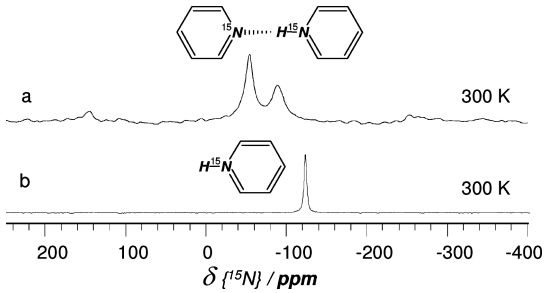

Figure 3. Solid state ^{15}N CPMAS NMR spectra of polycrystalline $[Pyr\text{-}H\cdots Pyr]^{+}$ $[BArF]^{-}$ (a) and $[Pyr\text{-}H]^{+}$ $[BArF]^{-}$ (b) at 300 K.

Figure 2 depicts low-temperature ^{15}N NMR spectra of $[Pyr\text{-}H\cdots Pyr]^{+}$. Again, both the multiplicity and the chemical shift of the signal depend on temperature although weaker as compared to the ^{1}H NMR spectra. Below 150 K, the signal is a doublet with a coupling constant of |40| Hz located at −62.7 ppm.

3.2. Solid State ^{15}N NMR. Figure 3a shows a $\{^{1}H\}$-^{15}N CPMAS spectrum of a polycrystalline $[Pyr\text{-}H\cdots Pyr]^{+}$ $[BArF]^{-}$ sample obtained at 300 K. There are two peaks at −88.8 and −53.8 ppm, Table 2. For comparison, in Figure 3b a spectrum of a polycrystalline $[Pyr\text{-}H]^{+}$ $[BArF]^{-}$ complex is depicted. Here the nitrogen resonates at −122.4 ppm.

3.3. XRD Crystal Structure. Variable temperature X-ray diffraction investigations show that $[Pyr\text{-}H\cdots Pyr]^{+}$ $[BArF]^{-}$ undergoes a phase transition at 190 ± 3 K. At the phase transition point the sample acts as a so-called "hopping crystal".[58] This is probably due to the large energy gap between the two phases. In view of the considerable disorder of the fluorine atoms, it may be assumed that the phase transition is associated with a freezing of the rotational motions of the CF_3 groups. Because of the large number of those groups the macroscopic single crystal structure may get destroyed in this type of phase transition. When the monocrystal was attached with glue before the cooling it changes to a powder encapsulated in glue on the needle of the diffractometer. At 193 K, the N...N distance is 2.647(8) Å and the angle between the C_2 symmetry axes of pyridines is 173°. Ipso-angles of the pyridine moieties are 118.7(7) and 121.4(6)°. The XRD structures of $[Pyr\text{-}H\cdots Pyr]^{+}$ and $[BArF]^{-}$ are depicted in Figure 4.

dx.doi.org/10.1021/jp203543g |J. Phys. Chem. A 2011, 115, 8041–8048

Table 2. Experimental ^{15}N NMR Chemical Shifts and Estimated Nitrogen-Proton Distances of Hydrogen-Bonded Acid−Base Complexes[a]

complex	T, K	$\delta(^{15}N)$, ±0.5 ppm	r_{NH} Å	ref
Bz-Col	300	−34	1.60	66
4-NO_2−Bz-Col	300	−47	1.44	66
4-Cl-3-NO_2−Bz-Col	300	−75	1.23	66
3,5-di-NO_2−Bz-Col	300	−89	1.16	66
2-NO_2−Bz-Col	300	−95	1.13	66
[Pyr-H···Pyr]$^+$	300	−88.8	1.16	this work
[Pyr-H···Pyr]$^+$	300	−53.8	1.37	this work
[Pyr-H]$^+$	300	−122.4		this work

[a] Col = 2,4,6-trimethylpyridine, Bz = benzoic acid, $\delta(^{15}N)$ = isotropic ^{15}N chemical shift obtained from CPMAS NMR spectra and referenced relative to the corresponding heterocycle, r_{NH} = N...H distance extrapolated using data of ref 66.

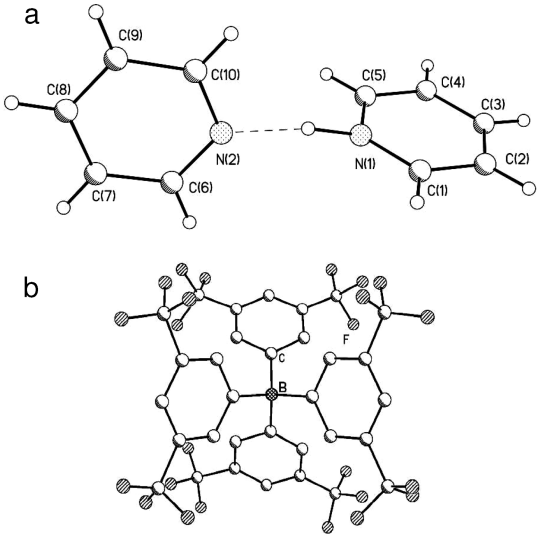

Figure 4. The general view of [Pyr-H···Pyr]$^+$ cation (a) and [BArF]$^-$ anion (b, hydrogen atoms are omitted for clarity) according to X-ray diffraction analysis.

3.4. INS Vibrational Spectra. The inelastic neutron scattering vibrational spectra of [Pyr-H···Pyr]$^+$ [BArF]$^-$ and [Pyr-D···Pyr]$^+$ [BArF]$^-$ are shown on the same intensity scale in Figure 5, and the simple difference spectrum {H−D} as open circles in the same plot. We note that the effect on the INS spectra of deuterium substitution for the H-bond proton is primarily to drastically reduce the intensities of those vibrational bands dominated by its motions. Vibrational modes involving the N−D···N hydrogen bond are essentially invisible since the scattering from D atoms is more than an order of magnitude less than that of H. The spectral difference therefore eliminates most of the vibrational modes of the Pyr and [BArF]$^-$ except those that may be strongly coupled to the protonic motions. The most notable differences in the H and D spectra are in the region of the in-plane bending mode δ(NH), that is, at about 1600−1700 cm^{-1}, and the out-of-plane bend γ(NH) at 822 cm^{-1}. Three additional peaks may be discerned in the difference spectrum at 568, 284, and 267 cm^{-1}, as well as some in the lattice region (not shown). Some relatively weak and broad bands are in evidence in the region above 2000 cm^{-1}, at approximately 2100 and 2450 cm^{-1}, essentially the same region where ν(OH) has been assigned[43] from solution IR spectra.

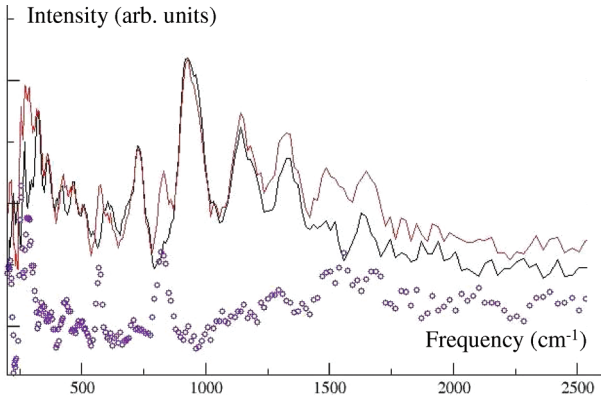

Figure 5. INS spectra of [Pyr-H···Pyr]$^+$ [BArF]$^-$ and [Pyr-D···Pyr]$^+$ [BArF]$^-$ on the same intensity scale, and their difference spectrum as open circles.

4. DISCUSSION

The structure (XRD) and spectral properties (^{1}H, ^{2}H, ^{15}N NMR, and INS vibration spectra) of [Pyr-H···Pyr]$^+$ in a complex with a poorly coordinating [BArF]$^-$ have been studied in the polar aprotic solvent $CDF_3/CDClF_2$ and in the crystalline state.

The [Pyr-H···Pyr]$^+$ hydrogen-bonded complex is stable in $CDF_3/CDClF_2$ below 150 K in both the ^{1}H and ^{15}N NMR time scales. The mobile proton resonates at 21.73 ppm that is above any value reported in the past.[59,60] Although, a part of this downfield shift should be attributed to the ring current effect.[61] The value of the primary isotope effect is close to the highest ever measured −0.95 ppm.[5,59,62] The dramatic low-field shift of the mobile proton resonance and the negative value of the effect proves that the hydrogen bond is very short, while the energy profile for the proton longitudinal vibration has two minima of the same depth. The multiplicity of the ^{1}H resonance indicates that the reversible proton transfer [Pyr-H···Pyr]$^+$ ⇌ [Pyr···H-Pyr]$^+$ is very fast down to 120 K. This finding correlates with the theoretical estimations that the barrier for the proton transfer is about 4 kJ/mol.[32] The rate limiting step for the proton transfer is the solvent reorganization.[8,9] The solvent molecules exhibit at a given time an asymmetry of the hydrogen bond and localize the proton at one of the bases. The observed coupling constant of |40| Hz is a result of averaging over two couplings: $^1J_{^{15}N^1H}$ and $^hJ_{^{15}N^1H}$. The former is the coupling across the N−H bond and the latter across the H···N bond. Thus, $(^1J_{^{15}N^1H} + {}^hJ_{^{15}N^1H})/(2)$ = |40| Hz. The value of $^1J_{^{15}N^1H}$ in an isolated [Pyr-H]$^+$ is negative and should be about −90 Hz.[63] We assign to the coupling the negative value taking into account results of theoretical calculations.[64] The value of $^hJ_{^{15}N^1H}$ is not necessarily negligible as compared to $^1J_{^{15}N^1H}$ but negative as well.[65] Thus, we conclude that $-80\ \text{Hz} \le {}^1J_{^{15}N^1H} < -40$ Hz. Indeed, computations predict for $^1J_{^{15}N^1H}$ a value of −69 Hz,[31] that is $^hJ_{^{15}N^1H}$ can be about −11 Hz. Remember that in the protonated homodimer of 2,4,6-trimethylpyridine the mobile proton resonates at 19.93 ppm, the primary isotope effect is −0.81 ppm, and $(^1J_{^{15}N^1H} + {}^hJ_{^{15}N^1H})/(2)$ = |40| Hz.[5]

A remarkable feature of the ^{1}H spectra of [Pyr-H···Pyr]$^+$ is the temperature dependence of the resonance position below

dx.doi.org/10.1021/jp203543g |J. Phys. Chem. A 2011, 115, 8041–8048

150 K, Figure 1d−f. The presence of a well resolved triplet in the spectra indicates that the proton exchange between different complexes is slow at these temperatures in the ^{1}H NMR time scale. That is the temperature dependence of the proton chemical shift cannot be a result of any exchange. We conclude that the geometry of $[\text{Pyr-H}\cdots\text{Pyr}]^+$ is temperature sensitive. The hydrogen bond becomes shorter, that is the length of the N−H distance increases, and the H···N and N...N distances contract upon cooling. The driving force for this strengthening is an increasing polarity of the solvent.[49] This effect has been predicted by quantum chemical calculations.[24] It has been interpreted in terms of a simple electrostatic model, accounting a decrease of the electrostatic repulsion of two negatively charged centers in a dielectric medium. The conclusion has been drawn that polar medium should cause some contraction of hydrogen bonds in ionic clusters combined with a decrease of the hydrogen bond asymmetry.[24] Remember that the static dielectric constant of $CDF_3/CDClF_2$ is about 24 at 150 K, 30 at 130 K, and 34 at 120 K.[49]

In the crystalline state, the proton of the $[\text{N}-\text{H}\cdots\text{N}]^+$ hydrogen bond is preferentially located at one of the nitrogens. As a result, $\{^1\text{H}\}$-^{15}N CPMAS spectra of polycrystalline $[\text{Pyr-H}\cdots\text{Pyr}]^+$ $[\text{BArF}]^-$ display two ^{15}N resonances. The peaks at −54 and at −89 ppm should be attributed to the H···^{15}N and to the ^{15}N−H nuclei, respectively.[66] According to XRD data at 193 K the N...N distances in $[\text{Pyr-H}\cdots\text{Pyr}]^+$ $[\text{BArF}]^-$ is 2.648 Å and the angle between the C_2 symmetry axes of pyridines is 173°.

4.1. Geometry of the $[\text{Pyr-H}\cdots\text{Pyr}]^+$ in the Crystalline State. The position of hydrogen atoms cannot be derived directly from the X-ray diffractions experiments.[67] However, the position of the mobile proton in $[\text{Pyr-H}\cdots\text{Pyr}]^+$ can be estimated indirectly using the influence of protonation on the C−N−C angle of pyridine. In free pyridine, this angle is about 118°, while upon protonation it increases up to 122°.[68] Our XRD data report for the angles at N(1) and N(2) the values of 121.5 and 118.8°, respectively, and we can unambiguously state that the mobile proton is located at the N(1) atom.

Special nontrivial efforts are needed to define the location of the mobile proton in hydrogen-bonded systems in the condense state. Only the qualitative trend can be reproduced using conventional quantum-mechanical calculation.[69] To overcome this problem, we have used a combined method. The coordinates of all atoms of the $[\text{Pyr-H}\cdots\text{Pyr}]^+$ moiety, except the position of the mobile proton, have been taken from the XRD experiment and kept frozen. The position of the mobile proton has been optimized at the B3LYP and MP2 levels using the 6-311++G** basis set of the Gaussian 98 program package.[70] The extremely tight threshold limits of 2×10^{-6} and 6×10^{-6} au have been applied for the maximum force and displacement as the convergence criteria, respectively. Both methods give essentially the same geometries. B3LYP/6-311++G** optimization results in an N−H distance of 1.123 Å, an H···N distance of 1.532 Å, and an NHN angle of 170.8°. MP2/6-311++G** optimization results in an N−H distance of 1.124 Å, an H···N distance of 1.531 Å, and an NHN angle of 171.0°. That is the total length of the hydrogen bond is 2.655 Å. This hydrogen bond is one of the shortest reported for the $[\text{Pyr-H}\cdots\text{Pyr}]^+$ system in the Cambridge Structural Database,[71] as is shown in the Supporting Information of this work. It is remarkable that the calculation of the geometry of an isolated proton-bound pyridine homodimer in the absence of any counterion results in an N−H distance of 1.119 Å, an H···N distance of 1.519 Å, and an NHN angle of 180.0°.[31] This coincidence provides one more prove that the poorly coordinating $[\text{BArF}]^-$ does not affect the geometry of $[\text{Pyr-H}\cdots\text{Pyr}]^+$.

In the past, some of us have shown that the isotropic ^{15}N chemical shift ($\delta(^{15}\text{N})$) of the hydrogen-bonded 2,4,6-trimethylpyridine (collidine) depends in a characteristic way on the nitrogen−hydrogen distance.[66] Only one of the principal components of the ^{15}N chemical shift anisotropy tensor is remarkably affected by a contraction of the distance. As a result, $\delta(^{15}\text{N})$ changes monotonically with the distance. On the basis of these findings, a correlation between the isotropic ^{15}N chemical shift and the nitrogen−hydrogen distance has been established.[66] It is of the essence that the difference between the limiting values of $\delta(^{15}\text{N})$ of a free heterocycle and its protonated cation is very the same for a number of symmetrically substituted pyridine derivatives, about −125 ppm.[63,66] It has been concluded that this correlation is appropriate to estimate hydrogen bond geometries using pyridine and its symmetrically substituted derivatives. In fact, it has been successfully done for a number of complex systems.[72−74]

Polycrystalline $[\text{Pyr-H}\cdots\text{Pyr}]^+$ $[\text{BArF}]^-$ offers us a unique opportunity to assess the feasibility of using this correlation to describe charged systems. Since $\delta(^{15}\text{N})$ values of both nitrogens are known we can estimate independently the N−H and the H···N distances. Selected values of $\delta(^{15}\text{N})$ and the corresponding N...H distances in hydrogen-bonded complexes of collidine with benzoic acid derivatives are collected in Table 2.[66] Let us apply the same correlation to $[\text{Pyr-H}\cdots\text{Pyr}]^+$. Then, the length of the N−H distance is about 1.16 Å and the length of the H···N distance is about 1.37 Å. Thus, there is a discrepancy between the values estimated on the base of XRD and NMR data. Of cause, one should take into account that these values have different physical meanings. The distances estimated quantum chemically on the base of XRD correspond to the minimum of the energy. The distances estimated from the NMR data correspond to the vibrationally averaged structures. For $[\text{Pyr-H}\cdots\text{Pyr}]^+$ this averaging leads to a lengthening of the N−H distance and a shortening of the H···N distance as compared to the most stable structure. Thus, the values obtained for the N−H distance using these two methods are in agreement. In contrast, it is obvious that the NMR correlation underestimates the length of the H···N distance. A part of this contraction is due to the vibrational averaging. The rest can be either ascribed to the fact that the correlation was established for neutral acid−base complexes, while the pyridine under discussion is hydrogen-bonded to a cation, or to the presence of a dynamic equilibrium between two energetically different forms $[\text{Pyr-H}\cdots\text{Pyr}]^+ \rightleftharpoons [\text{Pyr}\cdots\text{H-Pyr}]^+$.

4.2. INS Vibrational Spectra. The primary interest in obtaining INS vibrational spectra of this complex lies in the identification of the protonic modes, and their relationship to the H-bond geometry and potential energy surface, as well as the H-bond dynamics of similar systems. Previous experimental[43,44] and computational studies[75] on the $[\text{Pyr-H}\cdots\text{Pyr}]^+$ ion have reported rather conflicting assignments of the H-bond modes, which we hoped to clarify with the use of INS on account of its very high sensitivity to protonic motions. The mode of most interest in this context is the antisymmetric stretching mode ν(NH) as its frequency has been used as an approximate measure of the strength of the H-bond, at least in the case of nearly linear systems. It is also typically easiest to assign from IR spectra. Some systematics of ν(NH) and N...N distance were tabulated by

Novak for bonds with an N...N distance greater than about 2.8 Å.[76] It may be expected, however, that ν(NH) becomes increasingly difficult to assign when the H-bond is very short, as is the case for OH...O hydrogen bonds. One reason for this is that some OH (or NH) stretching component enters into many other molecular vibrational modes so that no single band can reliably be identified as "the" NH (or OH) stretching mode. This effect is in part related to the extreme anharmonicity of the potential energy surface for such short hydrogen bonds, which can shift ν(NH) to low enough frequencies[12] to facilitate such coupling to other vibrational modes.

Previous IR studies[43] of the $[Pyr\text{-}H\cdots Pyr]^+$ ion in solution have reported a broad doublet at approximately 2080 and 2530 cm^{-1}. A very recent work involving computation and IR spectra on the ion in the gas phase and solution observed a similar doublet for the N−H stretching band, but in addition the authors assigned a tunnel splitting in solution at 242 cm^{-1}, the symmetric H-bond stretching mode at 138 cm^{-1}, γ(NH) and δ(NH) at 1255 and 1655 cm^{-1}, respectively.[75] It should be noted, however, the H-bond for the $[Pyr\text{-}H\cdots Pyr]^+$ ion in solution was found to be considerably longer (calculated value of d(NN) = 2.763 Å)[75] than in the gas phase (d(NN) = 2.687 Å), which in turn is somewhat longer than in solid (present case, d(NN)= 2.655 Å).

The protonic mode, which usually easiest to assign from INS spectra (Figure 5), is the out-of-plane bending γ(NH), as does not mix strongly with other modes, and involves a large amplitude displacement of the proton, and it can clearly be identified in the present case at 822 cm^{-1}. Two bands involving the in-plane bending δ(NH) are discernible in the spectral difference at approximately 1550 and 1700 cm^{-1}, which is comparable to assignments in the IR solution spectra. Our INS spectra also show some weak evidence for two broad bands in the region above 2000 cm^{-1}, at approximately 2100 and 2450 cm^{-1}, essentially the same region where these would be expected according to published correlations,[76] and where they have been observed in solution IR spectra. The above tentative assignments of protonic modes in the INS spectra do, however, leave several prominent bands in the spectral difference at lower frequency, most notably at 568, 284, and 267 cm^{-1}, to be accounted for. The first of these may be assigned to pyridine ring deformation (ν_{10}), usually observed near 596 cm^{-1},[77] which involves a considerable displacement of the NH proton along the NH stretching coordinate. The two remaining bands in the difference spectrum at 267 and 284 cm^{-1} are not close in frequency to any internal mode in pyridine, so we are left to suggest that a full periodic calculation of the present system $[Pyr\text{-}H\cdots Pyr]^+$ $[BArF]^-$ would be required to identity these modes. A tunneling mode as assigned at 242 cm^{-1} by Tayyaru et al.[75] in solution would not be expected in the present case with an obviously highly asymmetric PES.

5. CONCLUSIONS

In this study, we have examined the structure and spectral signatures of a benchmark system of very strong asymmetric hydrogen bonds, the protonated homodimer of pyridine, $[Pyr\cdots H\cdots Pyr]^+$. A bulky poorly coordinating tetrakis[3, 5-bis(trifluoromethyl)phenyl]-borate ($[BArF]^-$) has been used as the counteranion to minimize the distortion of the hydrogen bond. The resulting complex is soluble in the polar freon mixture $CDF_3/CDClF_2$, that remains liquid down to 100 K and provides the possibility to inspect the features of $[Pyr\cdots H\cdots Pyr]^+$ in solution in the slow intermolecular exchange regime. Both the multiplicity of the ^1H resonance and the high negative primary isotope effect of −0.95 ppm indicate that the reversible proton transfer $[Pyr\text{-}H\cdots Pyr]^+ \rightleftharpoons [Pyr\cdots H\text{-}Pyr]^+$ is fast in the NMR time scale down to 120 K. Thus, the hydrogen bond is asymmetric, although quite short as the mobile proton resonates at 21.73 ppm that is above any value reported in the past.

Besides that we have also succeeded to obtain single crystals of $[Pyr\text{-}H\cdots Pyr]^+$ $[BArF]^-$ of a size suitable for high-resolution X-ray diffraction analysis. By combining the obtained data with model computations at the B3LYP/6-311++G** and MP2/6-311++G** levels, we have defined the position of the mobile proton as d(N−H) = 1.123 Å and d(H···N) = 1.532 Å. The same distances have been estimated using a ^{15}N NMR based correlation. Despite some deviations, the latter correlation provides a very reliable estimation for the N−H distance but underestimates the length of the H···N distance by 10%. Such a small difference is surprising as the correlation had been established for neutral O···H···N hydrogen bonds.

The inelastic neutron scattering {H−D}-bond spectral difference provides relatively unambiguous assignments of the protonic vibrational modes, and agree reasonably well with previous IR studies as far as ν(NH) (2100 and 2450 cm^{-1}) and δ(NH) (1550 and 1700 cm^{-1}) are concerned, but clearly place the out-of-plane bending mode at 822 cm^{-1} in much better agreement with Novak's correlation.[76]

■ ASSOCIATED CONTENT

Ⓢ Supporting Information. X-ray diffraction structure for single crystal $[Pyr\text{-}H\cdots Pyr]^+$ $[BArF]^-$ at 193 K; N...N distances reported for $[Pyr\text{-}H\cdots Pyr]^+$ in the crystalline state in the Cambridge Structural Database.[71] This material is available free of charge via the Internet at http://pubs.acs.org.

■ AUTHOR INFORMATION

Corresponding Author

*E-mail: shender@chemie.fu-berlin.de. Tel.: +49 30 8385 3615.

■ ACKNOWLEDGMENT

This work was supported by the German-Russian Interdisciplinary Science Center (G-RISC) funded by the German Federal Foreign Office via the German Academic Exchange Service (DAAD), the Russian Foundation of Basic Research (Projects 09-03-91336 and 10-03-00578), and the contract 02.740.11.0214. This work has benefited from the use of the Manuel Lujan, Jr. Neutron Scattering Center at Los Alamos National Laboratory and funding from the U.S. Department of Energy's Office of Basic Energy Sciences. Los Alamos National Laboratory is operated by Los Alamos National Security LLC under DOE Contract DE-AC52-06NA25396. Work at UCSB was supported by the Office of Energy Efficiency and Renewable Energy, U. S. Department of Energy.

■ REFERENCES

(1) Kirby, A. J. *Acc. Chem. Res.* **1997**, *30*, 290–296.

(2) Chan, B.; Del Bene, J. E.; Radom, L. *Mol. Phys.* **2009**, *107*, 1095–1105.

(3) Chan, B.; Del Bene, J. E.; Radom, L. *J. Am. Chem. Soc.* **2007**, *129*, 12197–12197.
(4) Majerz, I.; Olovsson, I. *Acta Crystallogr.* **2007**, *B63*, 650–662.
(5) Filarowski, A. *J. Phys. Org. Chem.* **2005**, *18*, 686–698.
(6) Lyssenko, K. A.; Antipin, M.Yu. *Russ. Chem. Bull.* **2006**, *55*, 1–15.
(7) Schah-Mohammedi, P.; Shenderovich, I. G.; Detering, C.; Limbach, H.-H.; Tolstoy, P. M.; Smirnov, S. N.; Denisov, G. S.; Golubev, N. S. *J. Am. Chem. Soc.* **2000**, *122*, 12878–12879.
(8) Perrin, C. L. *Pure Appl. Chem.* **2009**, *81*, 571–583.
(9) Perrin, C. L.; Karri, P. *Chem. Commun.* **2010**, *46*, 481–483.
(10) Golubev, N. S.; Shenderovich, I. G.; Smirnov, S. N.; Denisov, G. S.; Limbach, H.-H. *Chem.—Eur. J.* **1999**, *5*, 492–497.
(11) Chapman, K.; Crittenden, D.; Bevitt, J.; Jordan, M. J. T.; Del Bene, J. E. *J. Phys. Chem.* **2001**, *105*, 5442–5449.
(12) Del Bene, J. E.; Jordan, M. J. T. *J. Mol. Struct. (THEOCHEM)* **2001**, *573*, 11–23.
(13) Manriquez, R.; Lopez-Dellamary, F. A.; Frydel, J.; Emmler, T.; Breitzke, H.; Buntkowsky, G.; Limbach, H.-H.; Shenderovich, I. G. *J. Phys. Chem. B* **2009**, *113*, 934–940.
(14) Desiraju, G. R. *Angew. Chem., Int. Ed.* **2007**, *46*, 8342–8356.
(15) Barnes, A. J.; Beech, T. R.; Mielke, Z. *J. Chem. Soc., Faraday Trans.* **1984**, *80*, 455–463.
(16) Vener, M. V. In *Hydrogen — Transfer Reactions*; Hynes, J. T., Klinman, J. P., Limbach, H. H., Schowen, R.L., Eds.; Wiley-VCH: Weinheim, 2007; Vol 2.
(17) Waddington, T. C. *Trans. Faraday Soc.* **1958**, *54*, 25–33.
(18) Larson, J. W.; McMahon, T. B. *J. Am. Chem. Soc.* **1983**, *105*, 2944–2950.
(19) Wenthold, P. G.; Squires, R. R. *J. Phys. Chem.* **1995**, *99*, 2002–2005.
(20) Almlöf, J. *Chem. Phys. Lett.* **1972**, *17*, 49–52.
(21) Kawaguchi, K.; Hirota, E. *J. Mol. Struct.* **1995**, *352/353*, 389–394.
(22) Fujiwara, F. Y.; Martin, J. S. *J. Am. Chem. Soc.* **1974**, *96*, 7625–7631.
(23) Shenderovich, I. G.; Smirnov, S. N.; Denisov, G. S.; Gindin, V. A.; Golubev, N. S.; Dunger, A.; Reibke, R.; Kirpekar, S.; Malkina, O. L.; Limbach, H.-H. *Ber. Bunsen-Ges. Phys. Chem.* **1998**, *102*, 422–428.
(24) Golubev, N. S.; Shenderovich, I. G.; Tolstoy, P. M.; Shchepkin, D. N. *J. Mol. Struct.* **2004**, *698*, 9–15.
(25) Panich, A. M. *Chem. Phys.* **1995**, *196*, 511–519.
(26) Vendrell, O.; Gatti, F.; Meyer, H.-D. *Angew. Chem., Int. Ed.* **2009**, *48*, 352–355.
(27) Kirchner, B. *ChemPhysChem* **2007**, *8*, 41–43.
(28) Chen, H.; Voth, G. A.; Agmon, N. *J. Phys. Chem.* **2010**, *114*, 333–339.
(29) Stoyanov, E. S.; Stoyanova, I. V.; Tham, F. S.; Reed, C. A. *J. Am. Chem. Soc.* **2008**, *130*, 12128–12138.
(30) Mohammed, O. F.; Pines, D.; Dreyer, J.; Pines, E.; Nibbering, E. T. J. *Science* **2005**, *310*, 83–86.
(31) Del Bene, J. E.; Elguero, J. *J. Phys. Chem. A* **2006**, *110*, 7496–7502.
(32) Shenderovich, I. G. *Russ. J. Gen. Chem.* **2007**, *77*, 620–625.
(33) Makowski, M.; Sadowski, R.; Augustin-Nowacka, D.; Chmurzynski, L. *J. Phys. Chem. A* **2001**, *105*, 6743–6749.
(34) Buckingham, A. D.; Del Bene, J. E.; McDowell, S. A. C. *Chem. Phys. Lett.* **2010**, *463*, 1–10.
(35) Cleland, W. W.; Kreevoy, M. M. *Science* **1994**, *264*, 1887–1890.
(36) Minshall, P. C.; Sheldrick, G. M. *Acta Crystallogr.* **1978**, *B34*, 1378–1380.
(37) Villarreal-Salinas, B. E.; Schlemper, E. O. *J. Cryst. Mol. Struct.* **1978**, *8*, 217–237.
(38) Katrusiak, A. *J. Mol. Struct.* **1999**, *474*, 125–133.
(39) Brencic, J. V.; Ceh, B.; Leban, I. *Acta Crystallogr.* **1979**, *B35*, 3028–3030.
(40) Drew, M. G. B.; McKee, V.; Nelson, S. M. *J.C.S. Dalton* **1978**, 80–84.
(41) Roziere, J.; Williams, J. M.; Grech, E.; Malarski, Z.; Sobcyzk, L. *J. Chem. Phys.* **1980**, *72*, 6117–6122.
(42) Teulon, P.; Delaplane, R. G.; Olovsson, I. *Acta Crystallogr.* **1985**, *C41*, 479–483.
(43) Clements, R.; Wood, J. L. *J. Mol. Struct.* **1973**, *17*, 265–282.
(44) Brzezinski, B.; Zundel, G. *J. Chem. Soc., Faraday Trans. 2* **1976**, *72*, 2127–2137.
(45) Sokolov, N. D.; Vener, M. V.; Savel'ev, V. A. *J. Mol. Struct.* **1990**, *222*, 365–386.
(46) Rabolt, A.; Bauer, R.; Zundel, G. *J. Phys. Chem.* **1995**, *99*, 1889–1895.
(47) Pietrzak, M.; Wehling, J. P.; Kong, S.; Tolstoy, P. M.; Shenderovich, I. G.; López, C.; Claramunt, R. M.; Elguero, J.; Denisov, G. S.; Limbach, H. H. *Chem. -Eur. J.* **2010**, *16*, 1679–1690.
(48) Lesnichin, S. B.; Tolstoy, P. M.; Limbach, H.-H.; Shenderovich, I. G. *Phys. Chem. Chem. Phys.* **2010**, *12*, 10373–10379.
(49) Shenderovich, I. G.; Burtsev, A. P.; Denisov, G. S.; Golubev, N. S.; Limbach, H. H. *Magn. Reson. Chem.* **2001**, *39*, S91–S99.
(50) Hayashi, S.; Hayamizu, K. *Bull. Chem. Soc. Jpn.* **1991**, *64*, 685–687.
(51) Witanowski, M.; Stefaniak, L.; Szymański, S.; Januszewski, H. *J. Magn. Reson.* **1977**, *28*, 217–226.
(52) SAINT-Plus; Bruker AXS Inc.: Madison, WI, 2001.
(53) Sheldrick, G. M. SADABS; Bruker AXS Inc.: Madison,WI, 1997.
(54) Sheldrick, G. M. *Acta Cryst.* **2008**, *A64*, 112–122.
(55) Taylor, A. D.; Wood, E. J.; Goldstone, J. A.; Eckert, J. *Nucl. Instrum. Methods* **1984**, *221*, 408.
(56) Limbach, H. H. In *NMR Basic Principles and Progress*; Springer-Verlag: Heidelberg, 1991; Vol. 23, pp 66−167.
(57) Sharif, S.; Shenderovich, I. G.; González, L.; Denisov, G. S.; Silverman, D. N.; Limbach, H.-H. *J. Phys. Chem. A* **2007**, *111*, 6084–6093.
(58) Bernstein, J. *Polymorphism in Molecular Crystals*; Clarendon Press: Oxford, 2002.
(59) Smirnov, S. N.; Golubev, N. S.; Denisov, G. S.; Benedict, H.; Schah-Mohammedi, P.; Limbach, H.-H. *J. Am. Chem. Soc.* **1996**, *118*, 4094–4101.
(60) Limbach, H.-H.; Tolstoy, P. M.; Perez-Hernandez, N.; Guo, J.; Shenderovich, I. G.; Denisov, G. S. *Israel J. Chem.* **2009**, *49*, 199–216.
(61) Shenderovich, I. G. *Russ. J. Gen. Chem.* **2006**, *76*, 501–506.
(62) Vener, M. V. *Chem. Phys.* **1992**, *166*, 311–316.
(63) Andreeva, D. V.; Ip, B.; Gurinov, A. A.; Tolstoy, P. M.; Shenderovich, I. G.; Limbach, H.-H. *J. Phys. Chem. A* **2006**, *110*, 10872–10879.
(64) Del Bene, J. E.; Alkorta, I.; Elguero, J. *J. Phys. Chem. A* **2009**, *113*, 12411–12420.
(65) Shenderovich, I. G.; Tolstoy, P. M.; Golubev, N. S.; Smirnov, S. N.; Denisov, G. S.; Limbach, H.-H. *J. Am. Chem. Soc.* **2003**, *125*, 11710–11720.
(66) Lorente, P.; Shenderovich, I. G.; Golubev, N. S.; Denisov, G. S.; Buntkowsky, G.; Limbach, H.-H. *Magn. Reson. Chem.* **2001**, *39*, S18–S29.
(67) Churchill, M. R. *Inorg. Chem.* **1973**, *12*, 1213–1214.
(68) Krygowski, T. M.; Szatyłowicz, H.; Zachara, J. E. *J. Org. Chem.* **2005**, *70*, 8859–8865.
(69) Kong, S.; Shenderovich, I. G.; Vener, M. V. *J. Phys. Chem. A* **2010**, *114*, 2393–2399.
(70) Frisch, M. J.; Trucks, G. W.; Schlegel, H. B.; Scuseria, G. E.; Robb, M. A.; Cheeseman, J. R.;Zakrzewski, V. G.; Montgomery, J. A.; Stratmann, Jr., R. E.; Burant, J. C.; Dapprich, S.; Millam, J. M.;Daniels, A. D.; Kudin, K. N.; Strain, M. C.; Farkas, O.; Tomasi, J.; Barone, V.; Cossi, M.; Cammi, R.;Mennucci, B.; Pomelli, C.; Adamo, C.; Clifford, S.; Ochterski, J.; Petersson, G. A.; Ayala, P. Y.; Cui,Q.; Morokuma, K.; Malick, D. K.; Rabuck, A. D.; Raghavachari, K.; Foresman, J. B.; Cioslowski, J.;Ortiz, J. V.; Baboul, A. G.; Stefanov, B. B.; Liu, G.; Liashenko, A.; Piskorz, P.; Komaromi, I.;Gomperts, R.; Martin, R. L.; Fox, D. J.; Keith, T.; Al-Laham, M. A.; Peng, C. Y.; Nanayakkara, A.;Challacombe, M.; Gill, P. M. W.; Johnson, B.; Chen, W.; Wong, M. W.; Andres, J. L.; Gonzalez, C.;Head-Gordon, M.; Replogle, E. S.; Pople, J. A. *Gaussian 98*, Revision A.7; Gaussian, Inc.: Pittsburgh, PA, 1998.
(71) Cambridge Crystallographic Database, release 2010.
(72) Mauder, D.; Akcakayiran, D.; Lesnichin, S. B.; Findenegg, G. H.; Shenderovich, I. G. *J. Phys. Chem. C* **2009**, *113*, 19185–19192.

(73) Ip, B. C. K.; Andreeva, D. V.; Buntkowsky, G.; Akcakayiran, D.; Findenegg, G. H.; Shenderovich, I. G. *Microporous Mesoporous Mater.* **2010**, *134*, 22–28.
(74) Sharif, S.; Fogle, E.; Toney, M. D.; Denisov, G. S.; Shenderovich, I. G.; Buntkowsky, G.; Tolstoy, P. M.; Chan Huot, M.; Limbach, H.-H. *J. Am. Chem. Soc.* **2007**, *129*, 9558–9559.
(75) Tayyari, S. F.; Mahdizadeh, S. J.; Holakoei, S.; Wang, Y. A. *J. Mol. Struct.* **2010**, *971*, 39–46.
(76) Novak, A. *Struct. Bonding* **1974**, *18*, 177–216.
(77) Urena, P. C. F.; Gomez, F. M.; Gonzalez, L. J. J.; Torres, M. E. *Spectrochim. Acta, Part A* **2003**, *59*, 2815–2839.